

Audrey Carrière,^{1,2,3,4} Yannick Jeanson,^{1,2,3,4} Sandra Berger-Müller,^{1,2,3,4} Mireille André,^{1,2,3,4} Vanessa Chenouard,^{1,2,3,4} Emmanuelle Arnaud,^{1,2,3,4} Corinne Barreau,^{1,2,3,4} Romy Walther,^{1,2,3,4} Anne Galinier,^{1,2,3,4} Brigitte Wdziekonski,⁵ Phi Villageois,⁵ Katie Louche,⁶ Philippe Collas,⁷ Cédric Moro,⁶ Christian Dani,⁵ Francesc Villarroya,⁸ and Louis Casteilla^{1,2,3,4}



Browning of White Adipose Cells by Intermediate Metabolites: An Adaptive Mechanism to Alleviate Redox Pressure

Diabetes 2014;63:3253–3265 | DOI: 10.2337/db13-1885

The presence of brown adipose tissue (BAT) in human adults opens attractive perspectives to treat metabolic disorders. Indeed, BAT dissipates energy as heat via uncoupling protein (UCP)1. Brown adipocytes are located in specific deposits or can emerge among white fat through the so-called browning process. Although numerous inducers have been shown to drive this process, no study has investigated whether it could be controlled by specific metabolites. Here, we show that lactate, an important metabolic intermediate, induces browning of murine white adipose cells with expression of functional UCP1. Lactate-induced browning also occurs in human cells and in vivo. Lactate controls *Ucp1* expression independently of hypoxia-inducible factor-1 α and PPAR α pathways but requires active PPAR γ signaling. We demonstrate that the lactate effect on *Ucp1* is mediated by intracellular redox modifications as a result of lactate transport through monocarboxylate transporters. Further, the ketone body β -hydroxybutyrate, another metabolite that impacts redox state, is also a strong browning inducer. Because this redox-dependent increase in *Ucp1* expression

promotes an oxidative phenotype with mitochondria, browning appears as an adaptive mechanism to alleviate redox pressure. Our findings open new perspectives for the control of adipose tissue browning and its physiological relevance.

Recent discoveries in adult humans have renewed the vision of brown adipose tissue (BAT) as a therapeutic target for treating metabolic disorders such as type 2 diabetes and obesity (1). Whereas white adipose tissue (WAT) represents the main energy store, BAT dissipates energy as heat by uncoupling the mitochondrial respiratory chain from ATP formation through expression of uncoupling protein (UCP)1 (2). Thus, BAT plays a key role in diet and nonshivering thermogenesis (3). While it was assumed for many years that in humans, BAT was only present in the neonate (with some exceptions such as cold-exposed workers or patients suffering from pheochromocytoma [4]), recent imaging studies revealed the presence of substantial deposits of UCP1-expressing adipocytes in human healthy adults, whose activity is negatively correlated with BMI (5).

¹CNRS 5273, UMR STROMALab, Toulouse, France

²Université de Toulouse, Université Paul Sabatier, UMR 5273, Toulouse, France

³INSERM U1031, Toulouse, France

⁴Établissement Français du Sang Pyrénées-Méditerranée, Toulouse, France

⁵Faculté de Médecine, Institut de Biologie Valrose CNRS/INSERM/Université Nice Sophia Antipolis, Nice, France

⁶INSERM, UMR 1048, Obesity Research Laboratory, Institute of Metabolic and Cardiovascular Diseases, Toulouse, France

⁷Stem Cell Epigenetics Laboratory, Institute of Basic Medical Sciences, Faculty of Medicine, and Norwegian Center for Stem Cell Research, University of Oslo, Oslo, Norway

⁸Departament de Bioquímica i Biologia Molecular and Institute of Biomedicine, Universitat de Barcelona, and CIBER Fisiopatología de la Obesidad y Nutrición, Barcelona, Spain

Corresponding author: Louis Casteilla, louis.casteilla@inserm.fr.

Received 13 December 2013 and accepted 22 April 2014.

This article contains Supplementary Data online at <http://diabetes.diabetesjournals.org/lookup/suppl/doi:10.2337/db13-1885/-/DC1>.

A.C. and Y.J. contributed equally to this work.

© 2014 by the American Diabetes Association. Readers may use this article as long as the work is properly cited, the use is educational and not for profit, and the work is not altered.

See accompanying article, p. 3175.

Certain WAT depots are readily able to convert to a “brown-like” state with prolonged cold exposure or treatment with β -adrenergic compounds (6,7). Several hormones, enzymes, transcription factors, and microRNAs have recently been shown to drive the emergence of inducible brown adipocytes in WAT (8). As increase clearance and use of nutrients by brown adipocytes reduce the excess of triglycerides and glucose and confer beneficial metabolic effects and/or protection from obesity in mice (9–11), increasing the activity and/or emergence of UCP1-positive cells holds promise for the treatment of metabolic diseases.

The influence of the metabolic environment on the browning process is to date poorly understood. Both white and brown adipose cells express metabolite receptors and transporters, which may act as sensors of their metabolic environment. Proton-linked monocarboxylate transporters (MCTs) (12), which drive lactate, pyruvate, and ketone body transport across plasma membranes, are present on the surface of rodent (13–15) and human (16) adipocytes. Notably, the MCT1 isoform, mainly involved in lactate import into cells, strongly increases in BAT after exercise (15). WAT adipocytes also express the G-protein-coupled receptors (GPRs) GPR81 and GPR109A, which are activated by lactate and the ketone body β -hydroxybutyrate (β HB), respectively (17).

Among intermediate metabolites, lactate mediates a large intercellular and interorgan metabolic interplay (18). Lactate uptake, which induces changes in cellular redox state, is associated with neoglucogenesis or ATP production (19). Whereas lactate has been considered for a long time as a glycolytic waste product, it acts as a metabolic fuel supporting organ (Cori cycle) and cell interactions between astrocytes and neurons (20), as well as between glycolytic and oxidative cancer cells (21). Furthermore, its role as a signaling molecule (termed “lactormone” [19]) has recently been shown (22–26).

Given recent evidence demonstrating that expression of MCT in adipose tissues is controlled by physiological stimuli of browning (15), we aimed to investigate whether lactate could directly regulate browning remodeling of white adipocytes. Here, we show that lactate strongly increases thermogenic gene expression in mouse and human white adipose cells, this effect being dependent on the presence of active peroxisome proliferator-activated receptor (PPAR) γ signaling. Importantly, we demonstrate that the lactate effect on *Ucp1* is mediated by intracellular redox modifications as a result of lactate transport through MCT. We also show that β HB, another metabolite having the same consequence on cellular redox state, is also a strong browning enhancer.

RESEARCH DESIGN AND METHODS

Animals

All studies were carried out using male C57BL/6J mice obtained from the Harlan Laboratory. *Ppar α* -null mice were obtained from The Jackson Laboratory (Bar Harbor, ME). Animals were housed in a controlled environment (12-h light/dark cycles at 21°C) with unrestricted access

to water and a standard chow diet (Usine d’Alimentation Rationnelle, Villemoisson sur Orge, France) in a pathogen-free animal facility (IFR150) and killed by cervical dislocation. All experimental procedures were done in compliance with French Ministry of Agriculture regulations for animal experimentation.

Primary Culture of Adipose-Derived Stem/Stromal Cells and Adipocyte Differentiation

White stromal vascular fractions from 6- to 8-week-old mice were obtained as previously described (27). After centrifugation, stromal vascular fraction cells resuspended in culture medium (α MEM plus 0.25 units/mL amphotericin, 100 units/mL penicillin, 100 mg/mL streptomycin, biotin, ascorbic acid, panthotenic acid, and 10% newborn calf serum) were plated and rinsed with PBS 3 h after plating. Remaining adherent adipose-derived stem/stromal cells were grown to confluence and exposed to the adipogenic cocktail containing 5 μ g/mL insulin, 2 ng/mL T3, 33.3 nmol/L dexamethasone, 10 μ g/mL transferrin, and 1 μ mol/L rosiglitazone in complete medium. Adipocytes differentiated for 7 days were treated with different compounds at the time and concentrations as indicated in the figure legends.

Maintenance and Differentiation of Human Adipocyte Progenitors

Human adipocyte progenitors were derived from induced pluripotent stem cells and cultivated as already described [28,29,29(a)]. For adipocyte differentiation, cells were cultured in proliferation medium, which was supplemented with 0.5 mmol/L isobutylmethylxanthine, 0.25 μ mol/L dexamethasone, 0.2 nmol/L T3, 1 μ g/mL insulin, and 1 μ mol/L BRL49653 once cells reached confluence.

Western Blot Analysis

We extracted proteins and performed Western blotting as previously described (30). Sources of antibodies are UCP1 (UCP11-A, diluted 1:2,000; Alpha Diagnostic), MCT4 (sc-50329, diluted 1:500; Santa Cruz Biotechnology) or actin (A5541, diluted 1:5,000; Sigma-Aldrich).

In Vivo Injection of Rosiglitazone and Lactate

Six-week-old mice were randomly divided into four groups and injected daily (200 μ L i.p.) with either 5% DMSO/lutrol F127 2% (BASF France, Levallois-Perret, France) and PBS 93% (v/v/v), rosiglitazone (250 μ g/mice), L-sodium lactate (375 μ mol/mice), and a combination of both molecules. After 11 days of injection and overnight fasting, mice were killed by cervical dislocation and inguinal and interscapular fat pads were harvested. Concerning UCP1 immunohistochemistry, mice were anesthetized by an injection of ketamine (100 mg/kg i.p.)-xylazine (10 mg/kg) before receiving an intracardiac perfusion of 3.6% formaldehyde. Total inguinal depots were removed, postfixed at 4°C overnight, and rinsed in PBS.

Immunohistochemistry

Sections of inguinal depots (200 μ m) or differentiated adipocytes cultivated in Lab-Teks were blocked and

permeabilized for 30 min at room temperature in PBS–2% horse serum–0.2% triton before incubation with sheep anti-UCP1 primary antibody (generous gift from Daniel Ricquier, Institut Cochin, Paris, France; Institut National de la Santé et de la Recherche Médicale, Paris, France; Centre National de la Recherche Scientifique, Paris, France; and Université Paris Descartes, Paris, France) diluted at 1:5,000. After washing steps, samples were incubated with Alexa Fluor 488 secondary antibody (Invitrogen, Cergy Pontoise, France). Adipocytes were visualized by staining lipid droplets with 4,4-difluoro-4-bora-3a,4a-diaza-s-indacene-3-dodecanoic acid (BODIPY) 558/568 C12 diluted at 1:2,000. Nuclei were stained with DAPI diluted at 1:10,000. Fluorescence analysis was performed using a multiphoton laser scanning microscope (Zeiss LSM 510 NLO confocal microscope equipped with a femtosecond Coherent pulsed laser).

Lactate and Glucose Measurements

Plasma and extracellular lactate levels were measured with the Lactate Pro test meter (Arkray). Glucose concentrations in cell supernatants were measured using Contour TS (Bayer). Values were normalized by cellular protein content of the feeder cell layer (differentiated adipocytes).

O₂ Consumption

The whole-cell layer of differentiated adipocytes was harvested and incubated in culture medium without serum and supplemented with 4% free fatty acid BSA in a magnetically stirred oxygen electrode chamber set to 37°C. Oxygen consumption was measured polarographically using a Clark oxygen electrode (Oxygraph-2k Oroboros). The chamber was closed, and the cells were incubated to determine the basal respiratory rate. Oligomycin (2 µg/mL) was then added to measure the coupled respiration rate and antimycin (20 µmol/L) was added to measure mitochondrial-derived oxygen consumption. Oxygen consumption rate was determined from the slope of a plot of O₂ concentration versus time.

NADH-to-NAD⁺ Ratio Assessment

NADH-to-NAD⁺ ratio was assessed by the EnzyChrom NAD⁺/NADH Assay kit (BioAssay Systems).

Glycerol Measurement

Samples of fresh supernatant of differentiated adipocytes were harvested, and glycerol was measured using the Triglycérides Enzymatiques PAP 150 (bioMérieux).

Nucleofection Procedure

At 80% confluence, murine adipose-derived stem/stromal cells were dissociated in 0.25% trypsin EDTA and numbered. For each nucleofection assay, 2×10^6 cells were nucleofected (Amaxa Cell line Nucleofector Kit V; Amaxa) with 1.6 µmol/L of scramble siRNA (AllStars Negative Control siRNA; Qiagen), *Mct1* siRNA (Mm_Slc16a1_2; Qiagen), or *Mct4* siRNA (Mm_Slc16a3_5; Qiagen) with the Nucleofector II device (X005 protocol). After 4 days of differentiation, cells were treated with 25 mmol/L lactate for 24 h.

RNA Extraction and Real-Time PCR

Total RNA from culture cells was isolated using an Qiagen RNeasy kit (Qiagen). For mouse tissues, total RNA was isolated by Qiazol extraction and purification was done using RNeasy minicolumns. For quantitative real-time PCR analysis, 300–1,000 ng total RNA was reverse transcribed using the High Capacity cDNA Reverse Transcription kit (Life Technologies/Applied Biosystem), SYBR Green PCR Master Mix (Life Technologies/Applied Biosystem), and 300 nmol/L primers on an Applied Biosystem StepOne instrument. Relative gene expression was calculated by the $\Delta\Delta CT$ method and normalized to *36B4* for mouse and *TBP* for human analysis. Primers are listed in Table 1.

Statistical Analyses

All results are expressed as mean \pm SEM from at least three individual experiments. Unpaired *t* test was used to calculate final *P* values.

RESULTS

Expression of MCTs in Brown Versus White Adipose Depots

As expected, higher expression of *Ucp1* was detected in BAT compared with white adipose depots (Fig. 1A). We compared the expression of *Mct1* and *Mct4*, the main MCTs enabling lactate uptake and export, respectively (21,22,31), in both brown and white adipose depots. Higher amount of *Mct1* mRNA was found in BAT compared with WAT depots (Fig. 1B). Conversely, *Mct4* mRNA levels were greater in WAT, especially in the low *Ucp1*-expressing epididymal fat pad, compared with BAT (Fig. 1C). Furthermore, in mice exposed to 4°C for 1–7 days, we observed, in addition to the increase in *Ucp1* expression in both BAT and inguinal depots (Fig. 1D), an increase in the expression of the lactate-importing isoform *Mct1* (Fig. 1E) without any change in *Mct4* expression (Fig. 1F). In addition, we found that plasma lactate levels significantly rose after 24 h and 72 h of cold exposure and returned to basal levels after 7 days of cold exposure (Fig. 1G). These data show that brown and white adipose depots display different profiles for MCT expression and that in vivo browning induced by cold acclimation is associated with an increased lactate import system in adipose depots together with transient modification of plasma lactate levels.

Lactate Induces Thermogenic Gene Expression in Both Murine and Human Adipose Cells

We then directly assessed the effects of lactate on adipocyte biology. Acute 48-h treatment of differentiated adipocytes isolated from inguinal fat pad with lactate resulted in a robust increase of *Ucp1* mRNA levels together with an upregulation of the expression of additional key thermogenic genes such as *Cidea*, *Fgf21*, and *Hoxc9* without any significant effect on other genes involved in brown fat cells function such as *Ppargc1a*,

Prdm16, *Tbx1*, *Zic1*, and *Lhx8* (Fig. 2A). This effect is specific to *Ucp1*, as no change was observed for *Ucp2* (Fig. 2A). Lactate treatment also increased the expression of the mitochondrial marker *Cox7a1* as well as the fatty acid oxidation marker *Cpt1b* (Fig. 2A). While no effect was observed for *Fabp4* or *Lpl* adipogenic genes, lactate significantly increased the expression of the nuclear receptor *Pparg*, a master regulator of both white and brown adipogenesis (Fig. 2A). The increase of *Ucp1* mRNA levels by lactate was associated with an increase in UCP1 content as shown by Western blot (Fig. 2B) (in a dose-dependent manner, with an effect starting at 10 mmol/L [data not shown]) and by immunofluorescence (Fig. 2C), which showed that lactate increased both the number of UCP1-positive cells and the intensity of UCP1 staining per cell. While no difference was observed concerning basal respiratory rate (data not shown), we found a higher uncoupled respiration in lactate-treated

cells (respiration insensitive to oligomycin; $78 \pm 9.1\%$ in lactate-treated cells compared with $27.2 \pm 11\%$ in control cells [$P < 0.05$]), demonstrating the functionality of UCP1. Further highlighting the brown-like phenotype of lactate-treated adipocytes, we found higher glucose consumption rate in lactate-treated cells compared with control cells (1.12 ± 0.04 -fold increase compared with control cells [$P < 0.05$]).

Lactate-increased *Ucp1* expression was already observed after 24 h of treatment, in a dose-dependent manner (Fig. 2D), with an effect starting at 5 mmol/L and reaching its maximum at 25 mmol/L. This lactate-induced *Ucp1* gene expression was not due to osmotic perturbations, as mannitol did not upregulate *Ucp1* (data not shown). Importantly, lactate-mediated increase in thermogenic gene expression also occurred in human-induced pluripotent stem-derived adipocytes (29) (Fig. 2E), demonstrating lactate effect on human cells. Together, these

Table 1—List and sequences of primers

| Target name | Forward primer | Reverse primer |
|------------------|-------------------------------|----------------------------|
| <i>m36b4</i> | AGTCGGAGGAATCAGATGAGGAT | GGCTGACTTGGTTGCTTTGG |
| <i>mUcp1</i> | GACCGACGGCCTTTTTCAA | AAAGCACACAAACATGATGACGTT |
| <i>mPparg</i> | AGTGTGAATTACAGCAAATCTCTGTTTT | GCACCATGCTCTGGGTCAA |
| <i>mPrdm16</i> | GCACTTGCTTAAATACATATCACGTGTT | CAGCTCGGAGGCCTTTTCT |
| <i>mPpargc1a</i> | TGATGACAGTGAAGATGAAAGTGATAAAC | GGCGACACATCGAACAAATGA |
| <i>mCidea</i> | CTAGCACCAAAGGCTGGTTC | CACGCAGTTCCCACACACTC |
| <i>mFabp4</i> | GATGCCTTTGTGGGAACCTG | GCCATGCCTGCCACTTTC |
| <i>mLpl</i> | GTGGCCGAGAGCGAGAAC | CCACCTCCGTGTAATCAAGAAG |
| <i>mVegf</i> | GGCCTCCGAAACCATGAA | GTGGAGGTACAGCAGTAAAGCCA |
| <i>mCox4i2</i> | GTTGACTGCTACGCCAGCGC | CCGGTACAAGGCCACCTTCTC |
| <i>mGlut1</i> | GGGCATGTGCTTCCAGTATGT | ACGAGGAGCACCGTGAAGAT |
| <i>mUcp2</i> | CTCAGAAAAGGTGCCTCCCGA | ATCGCCTCCCTGTTGATGTGGTCA |
| <i>mFgf21</i> | TACACAGATGACGACCAAGA | GGCTTCAGACTGGTACACAT |
| <i>mMct1</i> | GAGGTTCTCCAGTGCTGTG | TCCATACATGTCATTGAGGCG |
| <i>mMct4</i> | AGTGCCATTGGTCTCGTG | CATACTTGTAACCTTTGGTTGCATC |
| <i>mZic1</i> | AACCTCAAGATCCACAAAAGGA | CCTCGAACTCGCACTTGAA |
| <i>mLhx8</i> | GAGCTCGGACCAGCTTCA | TTGTTGCTCTGAGCGAACTG |
| <i>mHoxc9</i> | GCAGCAAGCACAAAGAGGAGAAG | GCGTCTGGTACTTGGTGTAGGG |
| <i>mCox7a1</i> | CAGCGTCATGGTCAGTCTGT | AGAAAACCGTGTGGCAGAGA |
| <i>mCox8b</i> | GAACCATGAAGCCAACGACT | GCGAAGTTCACAGTGGTTCC |
| <i>mElovl3</i> | TCCGCGTTCTCATGTAGGTCT | GGACCTGATGCAACCCTATGA |
| <i>mTbx1</i> | GAGGACTGGCCCCGGAA | TTGTCTGAGCCATTGGGCTG |
| <i>mPdk4</i> | CACATGCTCTTGAACCTTTCAAG | TGATTGTAAGGTCTTCTTTTCCCAAG |
| <i>mAcox</i> | CCTGAAGAAATCATGTGGTTTAAAAA | CAGGAACATGCCCAAGTGAA |
| <i>mCpt1b</i> | TGTCTACCTCCGAAGCAGGA | TGAACGGCATTGCCTAGACG |
| <i>mAdipoq</i> | TCCTGGAGAGAAGGGAGAGAAAAG | CCCTTCAGCTCCTGTCTATTCC |
| <i>hCIDEA</i> | AGTCTGTTGACCCCGCTC | GCTATTTCCCGACCTCTTCGG |
| <i>hPPARG</i> | AGCCTCATGAAGAGCCTTCCA | TCCGGAAGAAACCCTTGCA |
| <i>hUCP1</i> | GTGTGCCCAACTGTGCAATG | CCAGGATCCAAGTCGCAAGA |
| <i>hTBP</i> | ACGCCAGCTTCGGAGAGTTC | CAAACCGCTTGGGATTATATTCCG |

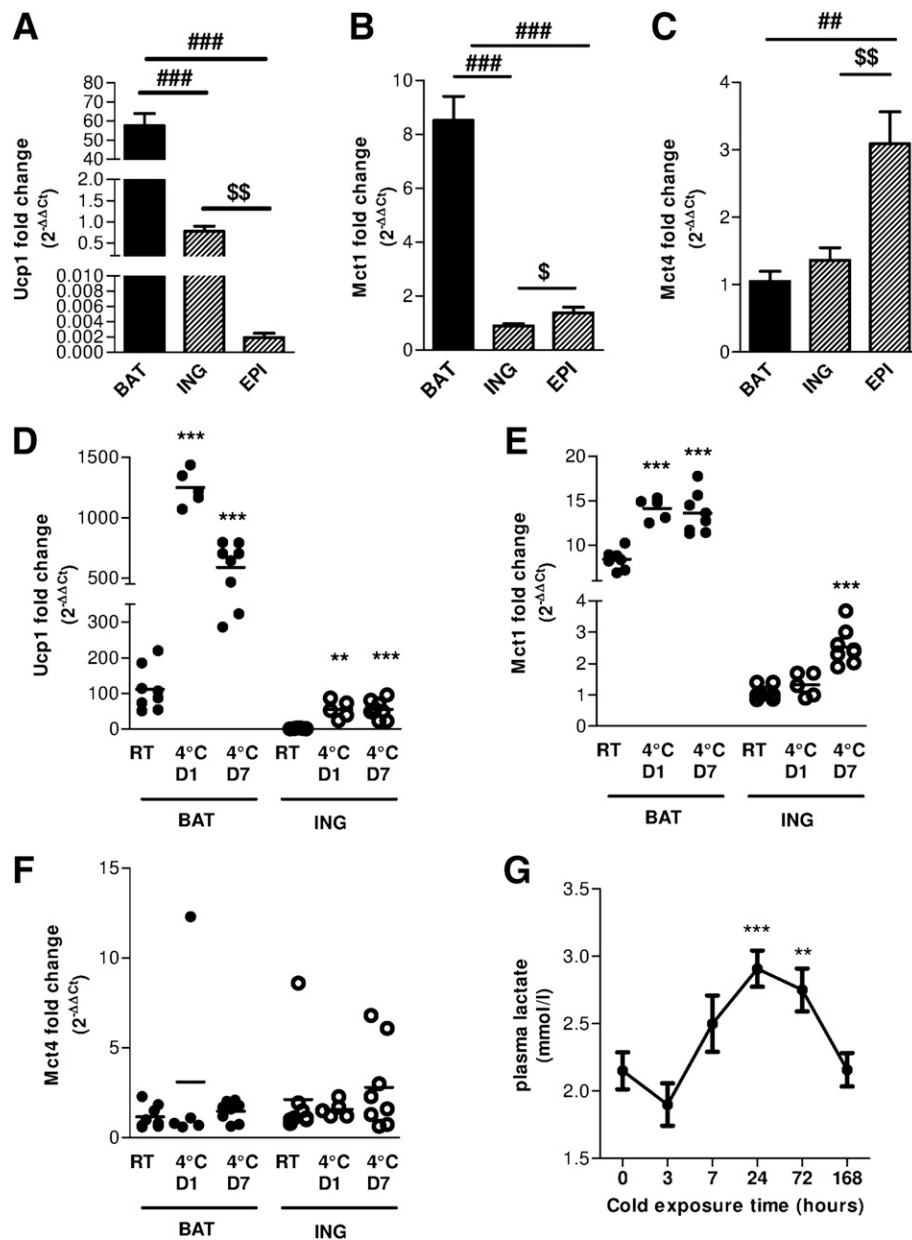


Figure 1—*Mct1* and *Mct4* expression in brown and white adipose depots during cold-induced browning. A–C: Interscapular BAT and inguinal (ING) and epididymal (EPI) white adipose depots were harvested from C57BL/6J mice. Total RNA was then isolated and assayed for mRNA levels of *Ucp1* (A) ($n = 6$), *Mct1* (B) ($n = 12$), and *Mct4* ($n = 12$) (C) by quantitative PCR (QPCR). D–F: BAT and ING white adipose depots of C57BL/6J mice exposed to 4°C for 1 ($n = 5$) or 7 ($n = 8$) days or maintained at room temperature (RT) (23°C) ($n = 8$) were harvested, and total RNA was isolated and assayed for mRNA levels of *Ucp1* (D), *Mct1* (E), and *Mct4* (F) by QPCR. G: C57BL/6J mice ($n = 12$) were exposed to 4°C for 3, 7, 24, 72, and 168 h. Lactate plasma concentrations were determined at each time point. $\#\#P < 0.01$, $\#\#\#P < 0.001$ vs. BAT; $\$P < 0.05$, $\$\$P < 0.01$ vs. inguinal white adipose depots; $\ast P < 0.01$, $\ast\ast\ast P < 0.001$ vs. RT.

data reveal that lactate is a strong inducer of brown adipose gene expression in white adipose cells, and this effect is conserved between species.

Induction of *Ucp1* by Lactate Is Distinct From Hypoxia-Inducible Factor-1 α and PPAR α Transduction Pathways but Requires an Active PPAR γ Signaling

During our investigation of lactate-regulated gene expression in white adipose cells, we observed an increase in the expression of *Glut1*, *Vegf*, and *Cox4i2* (Fig. 3A). These

genes are all targets of the hypoxia-inducible transcription factor hypoxia-inducible factor (HIF)-1 α (32,33), which has been shown to be stabilized by lactate (22). Our observation that DMOG, a prolyl-4-hydroxylase inhibitor that stabilizes HIF-1 α (32), increased *Glut1*, *Vegf*, and *Cox4i2* expression as expected but not *Ucp1* expression (and, rather, downregulated it [Fig. 3B]), together with the fact that incubation of white adipocytes under 1% O $_2$ for 24 h did not upregulate *Ucp1* expression (data

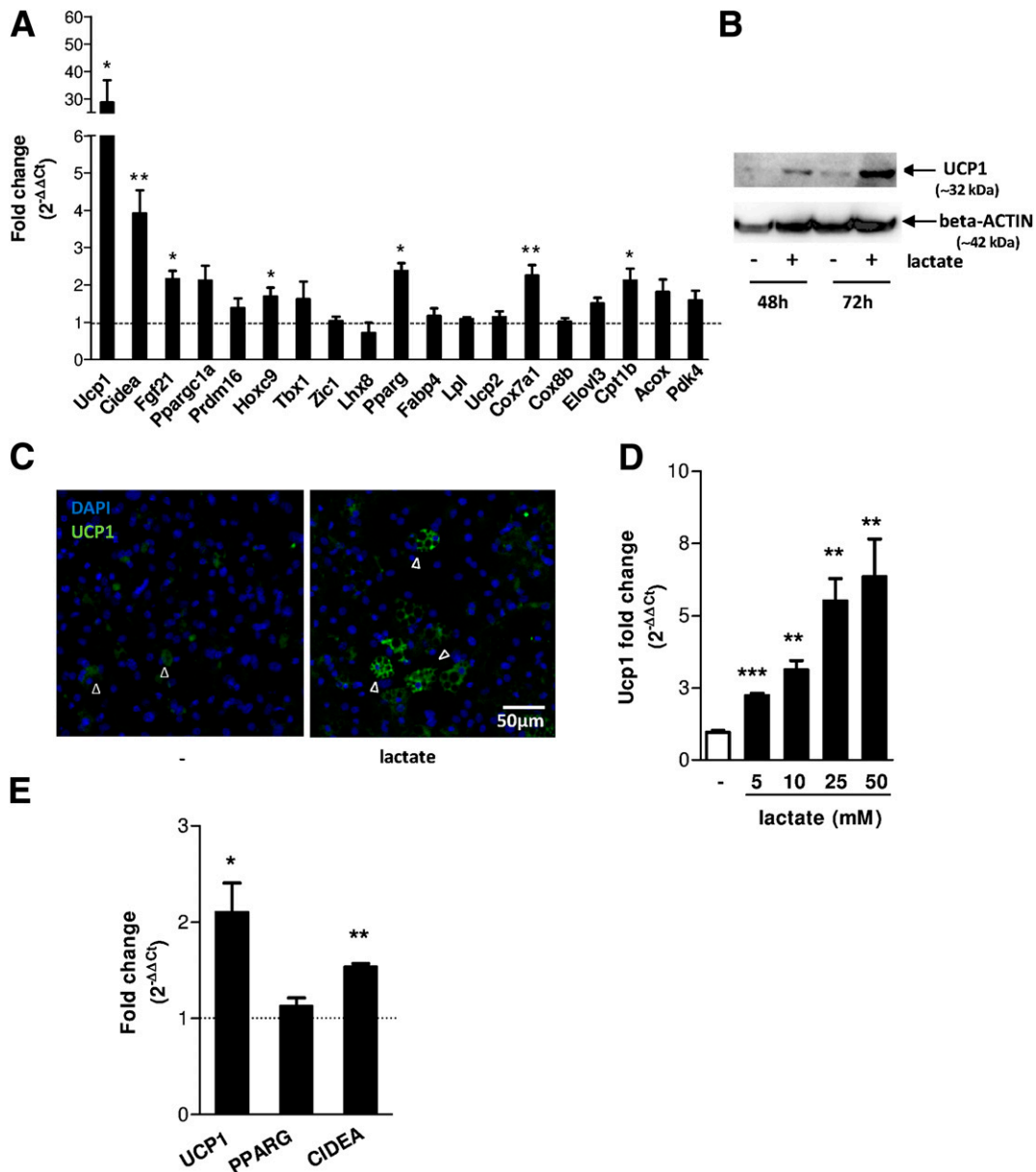


Figure 2—Lactate induces thermogenic gene expression in murine and human adipose cells. **A**: Mouse primary differentiated white adipocytes were treated with 50 mmol/L lactate for 48 h. Total RNA was then isolated and assayed for mRNA levels of *Ucp1*, *Cidea*, *Fgf21*, *Ppargc1a*, *Prdm16*, *Hoxc9*, *Tbx1*, *Zic1*, *Lhx8*, *Pparg*, *Fabp4*, *Lpl*, *Ucp2*, *Cox7a1*, *Cox8b*, *Elovl3*, *Cpt1b*, *Acox*, and *Pdk4* by quantitative PCR (QPCR). **B**: Western blot analysis of UCP1 expression in mouse primary differentiated white adipocytes treated with 50 mmol/L lactate for 48 and 72 h; β -ACTIN was used as loading control. **C**: Microscopy and multiphoton images of mouse primary differentiated white adipocytes treated with 50 mmol/L lactate for 48 h and stained with an antibody recognizing UCP1 (green) are shown; nuclei are stained by DAPI (blue). The arrows represent UCP1-positive adipocytes. **D**: Mouse primary differentiated white adipocytes were treated with increasing concentrations of lactate for 24 h. Total RNA was then isolated and assayed for mRNA levels of *Ucp1* by QPCR. **E**: Human-induced pluripotent stem-derived adipocyte cells were treated with 25 mmol/L lactate for 48 h. Total RNA was then isolated and assayed for mRNA levels of *UCP1*, *PPARG*, and *CIDEA* by QPCR. * $P < 0.05$, ** $P < 0.01$, *** $P < 0.001$ vs. control cells ($n = 3$ for each panel).

not shown), enabled us to exclude any role for HIF-1 α in the control of *Ucp1* expression by lactate. As *Ucp1* expression is regulated by PPAR α and PPAR γ signaling pathways, we tested their involvement in lactate effect. The increase in *Ucp1* expression by lactate similarly occurred in *Ppara* knockout versus wild-type adipocytes (Fig. 3C), ruling out a role of PPAR α . In contrast, *Ucp1* expression

in white adipose cells required the presence of the PPAR γ ligand rosiglitazone (as already demonstrated [34]), in both basal and lactate-treatment conditions (Fig. 3D) and is decreased by the PPAR γ antagonist GW9662 (Fig. 3E). As the expression of *Fabp4* and *Adipoq*, two well-described PPAR γ targets, was not upregulated by lactate treatment (Supplementary Fig. 1), we concluded that

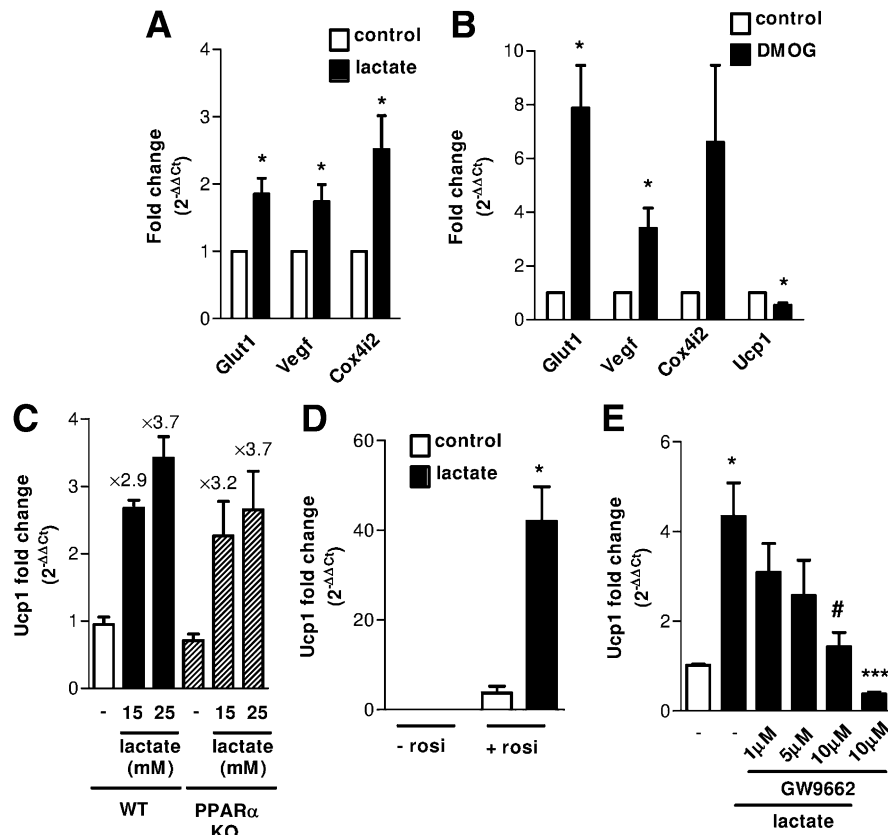


Figure 3—Induction of *Ucp1* by lactate is distinct from HIF-1 α and PPAR α transduction pathways but requires an active PPAR γ . Mouse primary differentiated white adipocytes were treated with 25 mmol/L lactate (A) and 1 mmol/L DMOG (B) (HIF-1 α stabilizing agent) for 24 h. Total RNA was then isolated and assayed for mRNA levels of *Glut1*, *Vegf*, *Cox4i2*, and *Ucp1* by quantitative PCR (QPCR) ($n = 4$). C: Mouse primary differentiated white adipocytes isolated from wild-type (WT) or *Ppara* knockout (KO) mice were treated with 15 and 25 mmol/L lactate for 24 h. Total RNA was then isolated and assayed for mRNA levels of *Ucp1* by QPCR ($n = 3$). D: Mouse primary white preadipocytes were differentiated in presence or not of rosiglitazone (rosi) for 6 days and then treated with or without 25 mmol/L lactate for 24 h. Total RNA was then isolated and assayed for mRNA levels of *Ucp1* by QPCR. *Ucp1* expression in cells that did not receive any rosiglitazone treatment was undetectable ($n = 3$). E: Mouse primary differentiated white adipocytes were preincubated for 45 min with increasing doses of the PPAR γ antagonist GW9662 (1, 5, and 10 μ mol/L) prior to lactate treatment (25 mmol/L for 24 h). Total RNA was then isolated and assayed for mRNA levels of *Ucp1* by QPCR ($n = 3$). * $P < 0.05$ and *** $P < 0.001$ vs. control cells, # $P < 0.05$ vs. lactate-treated cells.

lactate requires a functional PPAR γ signaling to regulate *Ucp1* expression but does not activate PPAR γ directly.

Lactate Induces Browning of WAT In Vivo

To determine whether lactate-induced browning also occurs in vivo, we treated mice with daily intraperitoneal injection of lactate for 11 consecutive days. As shown in Fig. 4A and B, lactate treatment by itself did not change *Ucp1* expression in inguinal or in interscapular brown adipose tissue (iBAT) fat pads. We then injected lactate in rosiglitazone-treated mice, as this antidiabetes compound had previously been shown to favor the browning process. As previously described (35), rosiglitazone-treated mice displayed an increase in *Ucp1* expression in inguinal (Fig. 4A), without any significant difference in *Ucp1* expression in iBAT (Fig. 4B). Strikingly, lactate coinjection with rosiglitazone further strongly enhanced both *Ucp1* and *Cidea* expression compared with rosiglitazone-injected mice (Fig. 4A) as well as mRNA levels of *Hoxc9*, *Cox7a1*, *Cpt1b*,

Acox, and *Pdk4* (Supplementary Fig. 2). This browning effect is specific to subcutaneous white adipose depot, as it did not occur in iBAT (Fig. 4B). The strong browning effect of lactate and rosiglitazone cotreatment on *Ucp1* expression was associated with a high increase in UCP1 content (Fig. 4C). High magnification shows that UCP1-positive cells are multilocular adipocytes, whereas unilocular adipocytes are UCP1 negative (Fig. 4D). Together, these data demonstrate that lactate induces the emergence of inducible brown adipocytes in white fat depots of mice treated with a PPAR γ agonist.

Lactate Transport Through MCTs Controls *Ucp1* Expression

To gain new insight into the mechanisms underlying lactate-induced *Ucp1* expression, we first investigated the role of the lactate receptor GPR81. Increasing doses of the GPR81 agonist 3,5-Dihydroxybenzoic acid did not affect *Ucp1* expression (Supplementary Fig. 3A), although this

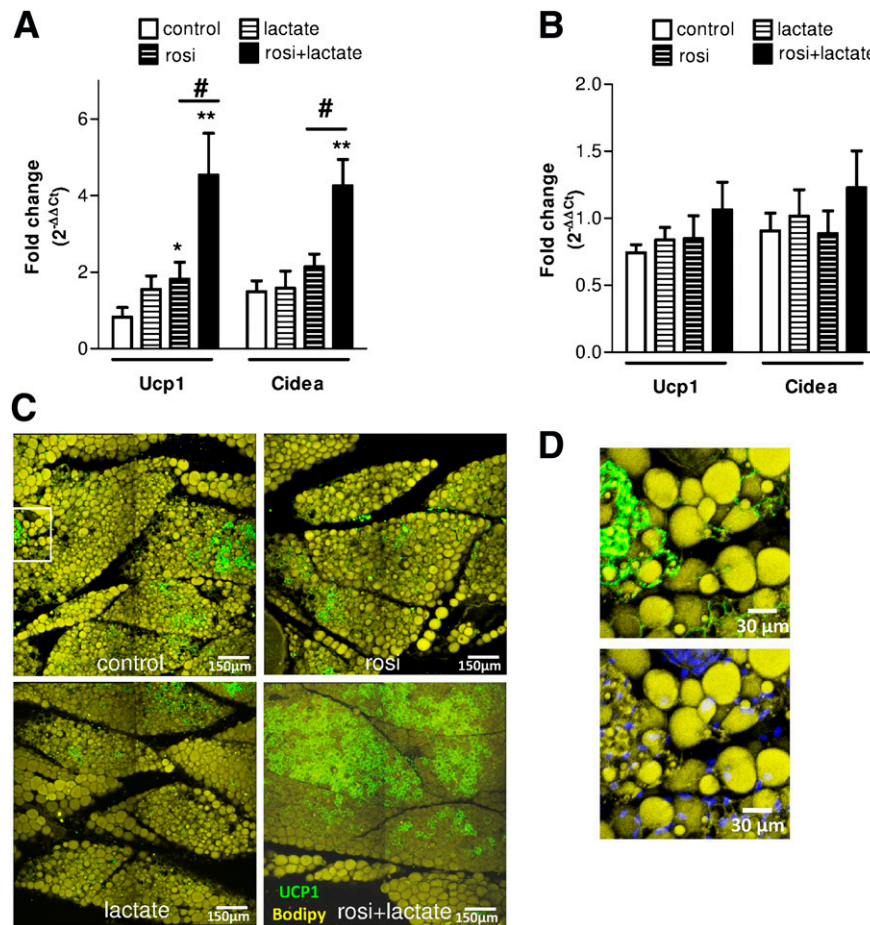


Figure 4—Lactate induces browning of WAT in vivo. *A–D*: C57BL/6J mice were daily and intraperitoneally injected with solvent (control mice, $n = 15$), lactate ($n = 14$), rosiglitazone (rosi) ($n = 11$), and a combination of rosiglitazone plus lactate ($n = 11$) during 11 consecutive days. Inguinal (*A*) and iBAT (*B*) fat pads were collected, and total RNA was isolated and assayed for mRNA levels of *Ucp1* and *Cidea* by quantitative PCR. * $P < 0.05$, ** $P < 0.01$ vs. control mice, # $P < 0.05$ vs. rosiglitazone-injected mice. *C*: Multiphoton images of inguinal and iBAT fat pads stained with an antibody recognizing UCP1 (green) and costained with the BODIPY lipid probe (yellow). *D*: High magnification of inguinal section of control mice (white rectangular from *C*) stained with an antibody recognizing UCP1 (green) and costained with the BODIPY lipid probe (yellow) is shown, and DAPI shows that UCP1-positive cells are multilocular adipocytes.

compound was effective in decreasing isoproterenol-induced lipolysis (Supplementary Fig. 3B), as already described (36). To address the putative involvement of MCT in lactate-mediated increase in *Ucp1* expression, we used two distinct MCT pharmacological inhibitors that have been shown to reduce lactate influx in several cell types (21,22,37). We found that both α -cyano-4-hydroxycinnamate and phloretin totally abrogated lactate-induced *Ucp1* expression (Fig. 5A). Interestingly, these inhibitors also decreased *Ucp1* expression in basal conditions (without extracellular lactate addition), suggesting that lactate endogenously produced and consumed by cells controls *Ucp1* expression. We then targeted *Mct1* and *Mct4* expression using an RNA interference approach. While downregulating *Mct1* expression induced no effect on *Ucp1* mRNA levels (data not shown), *Ucp1* expression was very sensitive to *Mct4* knockdown (consequences of *Mct4* knockdown are shown at mRNA levels [Fig. 5B], protein levels [Fig. 5C], and functional levels assessed by lactate measurement

in cell supernatants [Fig. 5D]). Indeed, reducing expression of the lactate-exporting MCT4 isoform strongly enhances *Ucp1* expression in both control and lactate-treated conditions (Fig. 5E), suggesting that intracellular lactate levels dictate *Ucp1* expression in white adipocytes. Altogether, these data show that lactate regulates *Ucp1* expression in adipocytes via MCT-mediated transport and in a GPR81-independent manner.

Redox Control of *Ucp1* Expression

Among the diverse consequences of increasing intracellular lactate levels through MCT, redox state (i.e., NADH-to-NAD⁺ ratio) might be changed through lactate conversion into pyruvate by the isoform B of the lactate dehydrogenase (Fig. 6A). We then tested the effect of the ketone body β HB, another monocarboxylate able to similarly affect redox state (Fig. 6A), on *Ucp1* expression. Strikingly, treatment of differentiated white adipocytes with β HB strongly increased expression of both *Ucp1* and *Cidea* in

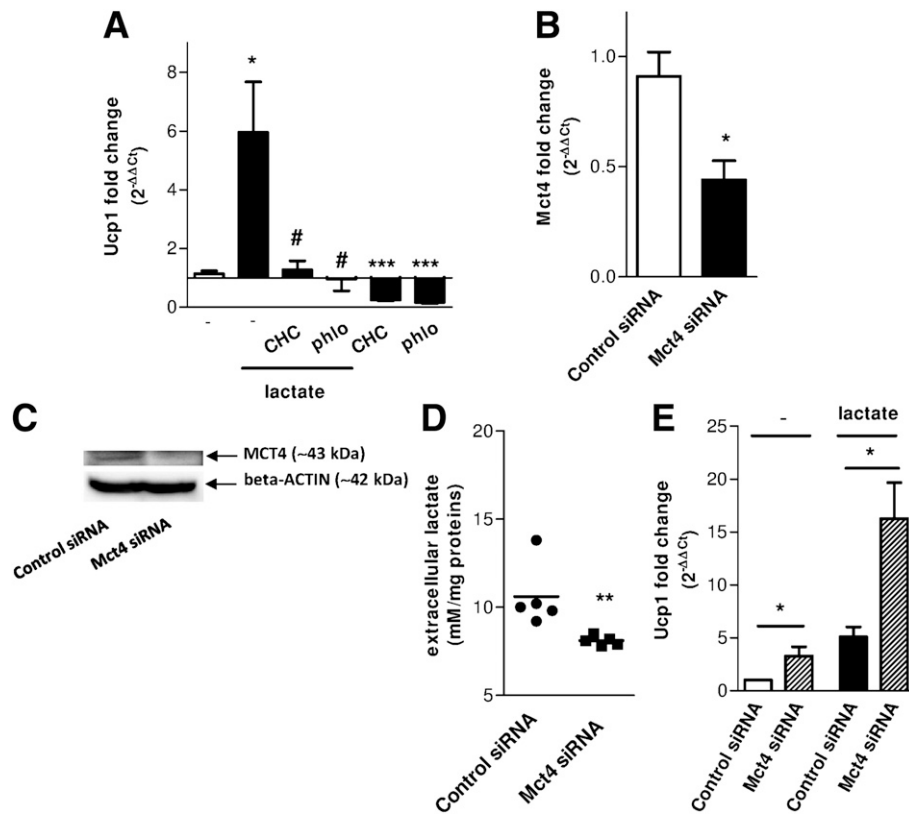


Figure 5—Lactate-induced *Ucp1* expression occurs through MCT transporters. **A**: Mouse primary differentiated white adipocytes were treated with or without 25 mmol/L lactate for 24 h in the presence of the MCT inhibitors α -cyano-4-hydroxycinnamate (CHC) (2 mmol/L) or phloretin (phlo) (50 μ mol/L). Total RNA was then isolated and assayed for mRNA levels of *Ucp1* by quantitative PCR (QPCR) ($n = 3$). **B–E**: Mouse primary white preadipocytes were transfected by electroporation with scramble control or *Mct4* siRNA. After 4 days of differentiation, cells were treated with or without 25 mmol/L lactate for 24 h. Total RNA was then isolated and assayed for mRNA levels of *Mct4* (**B**) and *Ucp1* (**E**) by QPCR ($n = 5$). Western blot analysis of MCT4 expression is shown in **C**, and extracellular lactate levels per milligram of protein are shown in **D** ($n = 5$). * $P < 0.05$ and *** $P < 0.001$ vs. control cells; ** $P < 0.01$ vs. control siRNA conditions; # $P < 0.05$ compared with lactate-treated cells.

a dose-dependent manner (Fig. 6B). In contrast, neither acetoacetate nor pyruvate displayed similar effects (Fig. 6C and D). The similar effect of lactate and β HB and the lack of effect of acetoacetate and pyruvate plus the increased NADH-to-NAD⁺ ratio in lactate- or β HB-treated adipocytes (Fig. 6E) clearly suggested a role for cellular redox state in the control of *Ucp1* expression. We then cotreated cells with lactate and increasing concentrations of pyruvate to modulate intracellular redox state according to the law of mass action (Fig. 6A). Clearly, addition of pyruvate significantly decreased lactate-induced *Ucp1* expression (Fig. 6F), as did the addition of acetoacetate in β HB-treated cells (Fig. 6G). Furthermore, addition of the uncoupling agent CCCP that decreases redox state by dissipating mitochondrial membrane potential abrogated both lactate- and β HB-induced *Ucp1* upregulation (Fig. 6H). Altogether, these data demonstrate that cellular redox change induced by lactate and β HB triggers their effect on *Ucp1* expression.

DISCUSSION

Although no metabolite has previously been shown to regulate the browning process, we demonstrate here that lactate drives the fate of white adipose murine and human

cells toward a brown and oxidative phenotype through sharp and rapid changes in the expression of several brown genes including *Ucp1*. We show that this lactate-based browning remodeling is mediated by intracellular redox modifications and that metabolites that similarly impact redox state such as the ketone body β HB also constitute strong browning inducers. We propose that under these conditions, induction of UCP1 constitutes an adaptive mechanism to alleviate redox pressure in adipocytes (Fig. 7).

Whereas lactate has been considered for a long time as a glycolytic waste product, its role as a true signaling molecule (termed “lactormone” [19]) has recently been emphasized. At physiological concentrations (from 10 mmol/L in plasma after acute exercise to 25 mmol/L [38] or even 40 mmol/L in muscle or certain tumors [39], respectively), lactate has been shown to specifically control gene expression in several cell types (22–26). Notably, lactate controls expression of several proteins involved in mitochondrial activity and biogenesis (24). Here, we show that lactate is also a strong enhancer of thermogenic gene expression. This effect starts at 5 mmol/L and is highly specific because it did not affect

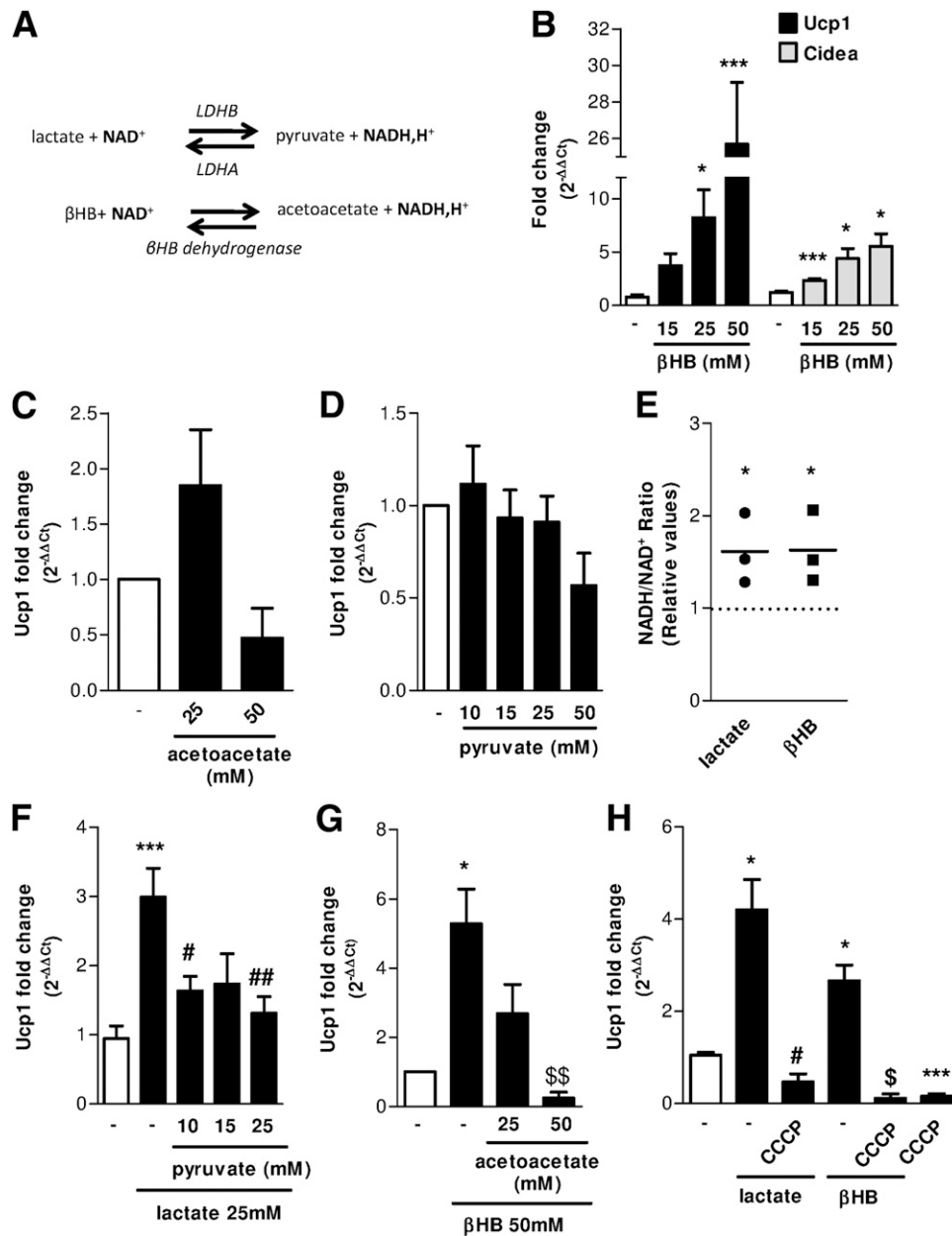


Figure 6—Redox control of *Ucp1* expression. **A**: Lactate-pyruvate and β HB-acetoacetate interconversions are catalyzed by lactate dehydrogenase and β HB dehydrogenase enzymes, respectively. These reactions tightly control the redox state, i.e., NADH-to-NAD⁺ ratio. **B**: Mouse primary differentiated white adipocytes were treated with 15, 25, and 50 mmol/L β HB for 24 h. Total RNA was then isolated and assayed for mRNA levels of *Ucp1* and *Cidea* by quantitative PCR (QPCR). Mouse primary differentiated white adipocytes were treated with increasing concentrations of acetoacetate (**C**) or pyruvate (**D**) for 24 h. Total RNA was then isolated and assayed for mRNA levels of *Ucp1* by QPCR. **E**: NADH-to-NAD⁺ ratio was assayed after 2 h of treatment with 50 mmol/L lactate or β HB on mouse primary differentiated white adipocytes. **F**: Mouse primary differentiated white adipocytes were treated with 25 mmol/L lactate for 24 h in the presence or not of 10, 15, or 25 mmol/L pyruvate. Total RNA was then isolated and assayed for mRNA levels of *Ucp1* by QPCR. **G**: Mouse primary differentiated white adipocytes were treated with 50 mmol/L β HB for 24 h in the presence or not of 25 or 50 mmol/L acetoacetate. Total RNA was then isolated and assayed for mRNA levels of *Ucp1* by QPCR. **H**: Mouse primary differentiated white adipocytes were treated with 25 mmol/L lactate or 25 mmol/L β HB for 24 h in the presence or not of a mitochondrial uncoupler (CCCP) (5 μ mol/L). Total RNA was then isolated and assayed for mRNA levels of *Ucp1* by QPCR. **P* < 0.05 and ****P* < 0.001 vs. control cells; #*P* < 0.05 and ##*P* < 0.01 vs. lactate-treated cells; \$*P* < 0.05 and \$\$*P* < 0.01 vs. β HB-treated cells (*n* = 3 for each panel).

Ucp2. Lactate can act through MCT transporters (12) and membrane receptors (17). In particular, lactate mediates the antilipolytic action of insulin through activation of the G_i-coupled receptor GPR81 by inducing a decrease

in cAMP levels (40). We show here that although activation of GPR81 inhibits isoproterenol-induced lipolysis as already described (36), it does not induce *Ucp1* expression. In any event, it is hardly conceivable that activation

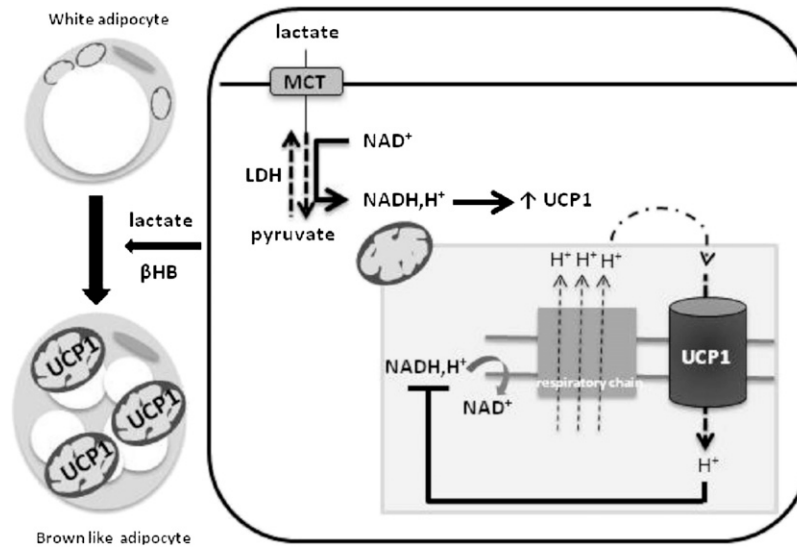


Figure 7—Model depicting the redox control of *Ucp1* expression. Induction of *Ucp1* by an increased redox state (NADH,H⁺-to-NAD⁺) favors its dissipation through increased uncoupled respiration. We propose that browning of white adipose cells by intermediate metabolites constitutes an adaptive mechanism to alleviate redox pressure. LDH, lactate dehydrogenase.

of G_i-coupled GPR81, which decreases cAMP levels, contributes to *Ucp1* expression given the cAMP-dependent regulation of *Ucp1* expression under noradrenergic stimulation. Conversely, we show by molecular and knock-down approaches that lactate transport through MCT is critical for the regulation of *Ucp1* expression. Whereas the two pharmacological inhibitors used, described as inhibitors of lactate import into several cell types (21,22,37), very efficiently reduce lactate-mediated *Ucp1* upregulation, downregulating *Mct1* displayed few effects on *Ucp1* levels; this, however, may be due to insufficient knock-down of the MCT1 protein and/or its high affinity for lactate (K_m ~3.5 mmol/L). In contrast, *Ucp1* expression is very sensitive to *Mct4* knockdown, as we found that reducing expression of the lactate exporting MCT4 isoform (which has a low affinity for lactate [K_m ~28 mmol/L]) strongly enhances *Ucp1* expression. The basal expression of *Ucp1* (without lactate addition) is very sensitive to both pharmacological inhibitors and *Mct4* knockdown, revealing an autocrine/paracrine mechanism by which lactate produced and consumed by cells tightly controls *Ucp1* expression. All these in vitro data are consistent with our in vivo findings demonstrating that 1) BAT displays higher *Mct1*-to-*Mct4* ratio compared with low *Ucp1*-expressing white adipose depots, 2) browning induced by cold acclimation is associated with an increase in the lactate-importing *Mct1* isoform that parallels *Ucp1* upregulation, and 3) plasma lactate levels showed a transient increase under cold-induced browning conditions.

We found that lactate increases expression of several HIF-1 α target genes, these findings being in total agreement with recent data demonstrating that lactate stabilizes HIF-1 α through its MCT-mediated intracellular transport

and direct inhibition of prolyl hydroxylase activity (22). However, we show that HIF-1 α signaling is not involved in *Ucp1* expression. We also show that lactate regulates *Ucp1* expression in a PPAR α -independent manner but required an active PPAR γ signaling pathway. In addition to these in vitro findings, we also show that the combination of lactate and the antidiabetes compound rosiglitazone constitutes a strong inducer of brown-like adipogenesis (and increased expression of some mitochondrial and β -oxidation markers), in white adipose depot, demonstrating that lactate controls the browning process in vivo.

After its transport inside the cell, lactate is converted into pyruvate by the lactate dehydrogenase following the reaction: lactate + NAD⁺ \rightleftharpoons pyruvate + NADH. Manipulation of the lactate-to-pyruvate ratio directly changes the cytoplasmic NADH-to-NAD⁺ ratio by the law of mass action. Spectacularly, the browning effect of lactate can be blunted with pyruvate; this undoubtedly demonstrates the key role of NADH-to-NAD⁺ ratio on *Ucp1* expression. Similar conclusions on the impact of NADH-to-NAD⁺ ratio can be drawn from the comparison between the effects of acetoacetate and β HB. Furthermore, it is remarkable that the uncoupling of mitochondria respiration by a chemical uncoupler mimicking UCP1 activity and thus consuming NADH alleviates the lactate-mediated increase in *Ucp1* expression. One can postulate that cells having high UCP1 activity and thus having a high capacity to dissipate redox pressure will become less responsive to lactate and β HB treatments than cells having low UCP1 expression and activity. Several protein sensors whose activities are dependent on the NADH-to-NAD⁺ ratio synchronize cell signaling and transcriptional events with the cellular metabolic state (41). Among them, some regulate

the expression of white and brown fat-selective gene programs such as the transcriptional coregulator COOH-terminal-binding protein-1 (CtBP-1) (42,43), as well as the NAD⁺-dependent Sirtuin-1 enzyme (44). Among the complex and redundant redox-sensitive signaling pathways, the identification of the lactate-redox-sensitive target(s) requires further investigations.

Our findings suggest that the browning remodeling of white adipose tissue, described in situations where such intermediate metabolites are released, could be due, at least partly, to their direct effects on adipose cells. Our *in vitro* imaging suggests that lactate-induced browning probably corresponds to both the emergence of new UCP1 positive cells and activation of preexisting low-UCP1-expressing cells. During exercise, beside the role of irisin (45), any increase in lactate could contribute to the browning remodeling. This is also in agreement with a recent demonstration that a ketone ester-enriched diet activates BAT and increases *Ucp1* expression in white adipose depot of C57BL/6J mice (46). It is also noteworthy that β HB constitutes a major energy metabolite for the newborn at a time where brown fat thermogenesis is crucial (47). Our findings bring very new insights in the browning field, as they demonstrate for the first time that specific metabolites have a drastic and direct impact on this phenomenon. Furthermore, because lactate or β HB promotes an oxidative phenotype with uncoupled mitochondria and elevated oxidation rate that in turn will decrease the redox pressure, browning remodeling of white adipose tissue and redox-dependent increase in *Ucp1* expression appears as an adaptive mechanism to alleviate redox pressure. This corresponds to an unexpected and new function for the development of these brown-like adipocytes and opens new perspectives for the control of adipose tissue browning and its physiological relevance.

Acknowledgments. This work is dedicated to Xavier Lerverve (Université de Grenoble) and, for our challenging and friendly discussions, to Michel Rigoulet (Institut de Biochimie et Génétique Cellulaires, UMR 5095, Université Bordeaux Segalen). We are grateful to Institut des Technologies Avancées en Sciences du Vivant (Unité Mixte de Service 3039) and to Institut des Maladies Métaboliques et Cardiovasculaires/UMR 1048, Plateforme Génome et Transcriptome du Génomole Toulouse. We especially thank Justine Caturla; Christophe Guissard, Clément Vecchi, and Pascale Guillou (UMR 5273 CNRS UPS EFS INSERM U1031); and Célia Bettiol (former student of UMR 5273 CNRS UPS EFS INSERM U1031) for excellent technical assistance.

Funding. This work was supported by the European Union FP7 project DIABAT (HEALTH-F2-2011-278373), the European Union FP7 project METABOSTEM (PCIG9-GA-2011-293720), and the ANR Safe.

Duality of Interest. No potential conflicts of interest relevant to this article were reported.

Author Contributions. A.C. designed the experiments, supervised experiments, researched and analyzed data, and wrote and edited the manuscript. Y.J. and S.B.-M. designed the experiments, researched and analyzed data, and reviewed the manuscript. M.A., V.C., E.A., C.B., R.W., A.G., B.W., P.V., and K.L. researched and discussed data. P.C., C.M., C.D., and F.V. contributed to the

experiments, discussed data, and reviewed the manuscript. L.C. designed the experiments, analyzed data, and wrote and reviewed the manuscript. A.C., Y.J., and L.C. are the guarantors of this work and, as such, had full access to all the data in the study and take responsibility for the integrity of the data and the accuracy of the data analysis.

References

- Algire C, Medrikova D, Herzig S. White and brown adipose stem cells: from signaling to clinical implications. *Biochim Biophys Acta* 2013;1831:896–904
- Nicholls DG, Locke RM. Thermogenic mechanisms in brown fat. *Physiol Rev* 1984;64:1–64
- Cannon B, Nedergaard J. Brown adipose tissue: function and physiological significance. *Physiol Rev* 2004;84:277–359
- Bouillaud F, Villarroya F, Hentz E, Raimbault S, Cassard AM, Ricquier D. Detection of brown adipose tissue uncoupling protein mRNA in adult patients by a human genomic probe. *Clin Sci (Lond)* 1988;75:21–27
- van Marken Lichtenbelt WD, Vanhommerig JW, Smulders NM, et al. Cold-activated brown adipose tissue in healthy men. *N Engl J Med* 2009;360:1500–1508
- Loncar D. Convertible adipose tissue in mice. *Cell Tissue Res* 1991;266:149–161
- Cousin B, Cinti S, Morroni M, et al. Occurrence of brown adipocytes in rat white adipose tissue: molecular and morphological characterization. *J Cell Sci* 1992;103:931–942
- Wu J, Cohen P, Spiegelman BM. Adaptive thermogenesis in adipocytes: is beige the new brown? *Genes Dev* 2013;27:234–250
- Bartelt A, Bruns OT, Reimer R, et al. Brown adipose tissue activity controls triglyceride clearance. *Nat Med* 2011;17:200–205
- Bartelt A, Heeren J. Adipose tissue browning and metabolic health. *Nat Rev Endocrinol* 2014;10:24–36
- Kopecky J, Clarke G, Enerbäck S, Spiegelman B, Kozak LP. Expression of the mitochondrial uncoupling protein gene from the α 2 gene promoter prevents genetic obesity. *J Clin Invest* 1995;96:2914–2923
- Halestrap AP. The SLC16 gene family - structure, role and regulation in health and disease. *Mol Aspects Med* 2013;34:337–349
- Hajduch E, Heyes RR, Watt PW, Hundal HS. Lactate transport in rat adipocytes: identification of monocarboxylate transporter 1 (MCT1) and its modulation during streptozotocin-induced diabetes. *FEBS Lett* 2000;479:89–92
- Iwanaga T, Kuchiiwa T, Saito M. Histochemical demonstration of monocarboxylate transporters in mouse brown adipose tissue. *Biomed Res* 2009;30:217–225
- De Matteis R, Lucertini F, Guescini M, et al. Exercise as a new physiological stimulus for brown adipose tissue activity. *Nutr Metab Cardiovasc Dis* 2013;23:582–590
- Pérez de Heredia F, Wood IS, Trayhurn P. Hypoxia stimulates lactate release and modulates monocarboxylate transporter (MCT1, MCT2, and MCT4) expression in human adipocytes. *Pflügers Arch* 2010;459:509–518
- Ahmed K, Tunaru S, Offermanns S. GPR109A, GPR109B and GPR81, a family of hydroxy-carboxylic acid receptors. *Trends Pharmacol Sci* 2009;30:557–562
- Lerverve XM, Mustafa I. Lactate: A key metabolite in the intercellular metabolic interplay. *Crit Care* 2002;6:284–285
- Brooks GA. Cell-cell and intracellular lactate shuttles. *J Physiol* 2009;587:5591–5600
- Pellerin L, Magistretti PJ. Sweet sixteen for ANLS. *J Cereb Blood Flow Metab* 2012;32:1152–1166
- Sonveaux P, Végran F, Schroeder T, et al. Targeting lactate-fueled respiration selectively kills hypoxic tumor cells in mice. *J Clin Invest* 2008;118:3930–3942
- Sonveaux P, Copetti T, De Saedeleer CJ, et al. Targeting the lactate transporter MCT1 in endothelial cells inhibits lactate-induced HIF-1 activation and tumor angiogenesis. *PLoS ONE* 2012;7:e33418

23. Végran F, Boidot R, Michiels C, Sonveaux P, Feron O. Lactate influx through the endothelial cell monocarboxylate transporter MCT1 supports an NF- κ B/IL-8 pathway that drives tumor angiogenesis. *Cancer Res* 2011;71:2550–2560
24. Hashimoto T, Hussien R, Oommen S, Gohil K, Brooks GA. Lactate sensitive transcription factor network in L6 cells: activation of MCT1 and mitochondrial biogenesis. *FASEB J* 2007;21:2602–2612
25. Formby B, Stern R. Lactate-sensitive response elements in genes involved in hyaluronan catabolism. *Biochem Biophys Res Commun* 2003;305:203–208
26. Samuvel DJ, Sundararaj KP, Nareika A, Lopes-Virella MF, Huang Y. Lactate boosts TLR4 signaling and NF-kappaB pathway-mediated gene transcription in macrophages via monocarboxylate transporters and MD-2 up-regulation. *J Immunol* 2009;182:2476–2484
27. Planat-Benard V, Silvestre JS, Cousin B, et al. Plasticity of human adipose lineage cells toward endothelial cells: physiological and therapeutic perspectives. *Circulation* 2004;109:656–663
28. Brown SE, Tong W, Krebsbach PH. The derivation of mesenchymal stem cells from human embryonic stem cells. *Cells Tissues Organs* 2009;189:256–260
29. Taura D, Noguchi M, Sone M, et al. Adipogenic differentiation of human induced pluripotent stem cells: comparison with that of human embryonic stem cells. *FEBS Lett* 2009;583:1029–1033
- 29(a). Mohsen-Kanson T, Hafner AL, Wdziekonski B, et al. Differentiation of human induced pluripotent stem cells into brown and white adipocytes: role of Pax3. *Stem Cells* 2014;32:1459–1467
30. Carrière A, Carmona MC, Fernandez Y, et al. Mitochondrial reactive oxygen species control the transcription factor CHOP-10/GADD153 and adipocyte differentiation: a mechanism for hypoxia-dependent effect. *J Biol Chem* 2004;279:40462–40469
31. Dimmer KS, Friedrich B, Lang F, Deitmer JW, Bröer S. The low-affinity monocarboxylate transporter MCT4 is adapted to the export of lactate in highly glycolytic cells. *Biochem J* 2000;350:219–227
32. Fukuda R, Zhang H, Kim JW, Shimoda L, Dang CV, Semenza GL. HIF-1 regulates cytochrome oxidase subunits to optimize efficiency of respiration in hypoxic cells. *Cell* 2007;129:111–122
33. Brahim-Horn MC, Bellot G, Pouysségur J. Hypoxia and energetic tumour metabolism. *Curr Opin Genet Dev* 2011;21:67–72
34. Petrovic N, Walden TB, Shabalina IG, Timmons JA, Cannon B, Nedergaard J. Chronic peroxisome proliferator-activated receptor gamma (PPARgamma) activation of epididymally derived white adipocyte cultures reveals a population of thermogenically competent, UCP1-containing adipocytes molecularly distinct from classic brown adipocytes. *J Biol Chem* 2010;285:7153–7164
35. Ohno H, Shinoda K, Spiegelman BM, Kajimura S. PPAR γ agonists induce a white-to-brown fat conversion through stabilization of PRDM16 protein. *Cell Metab* 2012;15:395–404
36. Liu C, Kuei C, Zhu J, et al. 3,5-Dihydroxybenzoic acid, a specific agonist for hydroxycarboxylic acid 1, inhibits lipolysis in adipocytes. *J Pharmacol Exp Ther* 2012;341:794–801
37. Kennedy KM, Dewhirst MW. Tumor metabolism of lactate: the influence and therapeutic potential for MCT and CD147 regulation. *Future Oncol* 2010;6:127–148
38. Philp A, Macdonald AL, Watt PW. Lactate—a signal coordinating cell and systemic function. *J Exp Biol* 2005;208:4561–4575
39. Walenta S, Schroeder T, Mueller-Klieser W. Lactate in solid malignant tumors: potential basis of a metabolic classification in clinical oncology. *Curr Med Chem* 2004;11:2195–2204
40. Ahmed K, Tunaru S, Tang C, et al. An autocrine lactate loop mediates insulin-dependent inhibition of lipolysis through GPR81. *Cell Metab* 2010;11:311–319
41. Chiarugi A, Dölle C, Felici R, Ziegler M. The NAD metabolome—a key determinant of cancer cell biology. *Nat Rev Cancer* 2012;12:741–752
42. Kajimura S, Seale P, Tomaru T, et al. Regulation of the brown and white fat gene programs through a PRDM16/CtBP transcriptional complex. *Genes Dev* 2008;22:1397–1409
43. Zhang Q, Wang SY, Nottke AC, Rocheleau JV, Piston DW, Goodman RH. Redox sensor CtBP mediates hypoxia-induced tumor cell migration. *Proc Natl Acad Sci USA* 2006;103:9029–9033
44. Qiang L, Wang L, Kon N, et al. Brown remodeling of white adipose tissue by SirT1-dependent deacetylation of Ppar γ . *Cell* 2012;150:620–632
45. Boström P, Wu J, Jedrychowski MP, et al. A PGC1- α -dependent myokine that drives brown-fat-like development of white fat and thermogenesis. *Nature* 2012;481:463–468
46. Srivastava S, Kashiwaya Y, King MT, et al. Mitochondrial biogenesis and increased uncoupling protein 1 in brown adipose tissue of mice fed a ketone ester diet. *FASEB J* 2012;26:2351–2362
47. Bougneres PF, Lemmel C, Ferré P, Bier DM. Ketone body transport in the human neonate and infant. *J Clin Invest* 1986;77:42–48